PCCP

RSC Publishing

PAPER

View Article Online
View Journal | View Issue

Cite this: *Phys. Chem. Chem. Phys.*, 2013, **15**, 972

Steady-state macroscale voltammetry in a supercritical carbon dioxide medium†

Kathryn E. Toghill,* Patrick Voyame, Dmitry Momotenko, Astrid J. Olaya and Hubert H. Girault*

Received 15th August 2012,
Accepted 24th October 2012

DOI: 10.1039/c2cp42856c

www.rsc.org/pccp

The electrochemical oxidation and reduction of decamethylferrocene is demonstrated in supercritical carbon dioxide at a macro gold disc electrode at 100 bar and 313 K. Fast mass transport effects were exhibited and the corresponding steady-state voltammetry was observed at high scan rates. A highly lipophilic room temperature ionic liquid that readily dissolved in supercritical CO_2 with acetonitrile as a co-solvent was used as an electrolyte, allowing for a conducting supercritical single phase. Experimental observations along with simulation results confirmed the hypothesis that a thin layer of liquid-like phase of co-solvent is formed at the electrode surface and is restricted by a more supercritical phase of high natural convection and bulk concentration.

Introduction

Supercritical CO_2 ($scCO_2$) has been a matter of interest to chemists for many decades, owing to variable properties that are neither liquid nor gaseous, highly tunable density changes and appealing solvating properties, particularly for solvent extraction. However, the very low relative permittivity of the fluid ($\varepsilon < 2$) has rendered the medium unsuitable for electrochemical processes due to a high electrical resistance. This is a frustrating property, as the electrochemical reduction of CO_2 to useful hydrocarbon fuels is an important area of research,[1] owing to the onset of global warming and the imminent depletion of fossil fuels. Despite this intrinsic resistivity, the use of fluorinated lipophilic salts and microelectrodes has allowed some degree of study in the non-conducting medium,[2–6] but on the whole, the literature is sparse. Voltammetry in $scCO_2$ fluids has seldom been reported, with the majority of publications utilizing ultramicroelectrodes[2,4,7] and conductive polymer coated electrodes.[3,8,9] On the macro scale the only publication known to date is that of Abbott and Harper.[5] However, the voltammetry presented was poorly defined and obtained at very slow scan rates, providing very little analytical insight.

The low dielectric constant for $scCO_2$ vastly limits the range of suitable electrolytes for electrochemical experiments. Conventional inorganic salts such as alkali chlorides remain completely insoluble in the fluid regardless of pressure and temperature. However, highly lipophilic salts that are generally used in non-aqueous electrochemistry can achieve considerably more solvation in $scCO_2$. Such electrolytes include tetrabutylammonium (TBA) cation with tetrafluoroborate (BF_4), perchlorate (P), hexafluorophosphate (PF_6), or bromide anions. Solubility is only attainable in the supercritical fluid in the presence of polar co-solvents, and even then most salts precipitate from the solution at the critical point, as observed by Chanfreau *et al.*[10] for TBAP in dimethylformamide–$scCO_2$ and by Jun and Fedkiw[11] for alkali metal perfluoroacetate salts in $scCO_2$–methanol systems.

In general, it is understood that the better electrolytes for $scCO_2$ electrochemistry are highly fluorinated salts and consist of bulky ions. Anions such as tetrakis(pentafluorophenyl)borate ($TFPB^-$) and tetrakis(3,5-trifluoromethyl phenyl)borate are often used in liquid–liquid electrochemistry to pump protons from a water phase into an organic phase,[12,13] but have also been applied to $scCO_2$ electrodeposition processes as reported recently by Bartlett *et al.*[14–16] In 1996, Abbott and co-workers[17] reported the high solubility of long chain ammonium alkanes in non-polar solvents, presenting tetra(decyl)ammonium tetraphenylborate (TDATPB) as a suitable electrolyte for $scCO_2$ studies.[5] Chanfreau *et al.* used the latter electrolyte more recently in the electrocarboxylation of benzyl chloride in pressurised CO_2.[18]

The recent interest in $scCO_2$ as a medium for electrodeposition and electroplating processes has revolved around the enhanced mass transport imparted by the low density fluid.[14–16,19] The enhancement is evident in these recent publications, yet an

Laboratoire d'Electrochimie Physique et Analytique (LEPA), Ecole polytechnique fédérale de Lausanne (EPFL), Institut des sciences et ingénierie chimiques (ISIC), Lausanne, Switzerland. E-mail: hubert.girault@epfl.ch; Fax: +41 (0)21 693 36 67; Tel: +41 (0)21 693 31 51

† Electronic supplementary information (ESI) available. See DOI: 10.1039/c2cp42856c

analytical study of mass transport effects, from a voltammetry perspective, and on the macro scale, has yet to be reported. In this paper we present a study of the metallocene, namely decamethylferrocene (DMFc), in a conventional three-electrode set-up at a macroscale gold electrode, using $scCO_2$ and acetonitrile as a polar co-solvent.

2. Experimental

2.1. Materials

Lithium tetrakis(pentafluorophenyl)borate ethyl etherate (LiTB purum) ($Li[B(C_6F_5)]_4$ $2.5C_4H_{10}O$) (Fluka, Switzerland) and tetradecyl ammonium bromide ($[N(C_{10}H_{11})_4]Br$) (Aldrich, Switzerland) were used as received without further purification. Analytical grade methanol (99.99%, Sigma, Switzerland), HPLC reagent grade (99.8%) 1,2-dichloroethane (Acros Organics, Origin) and GC reagent grade (99.5%) acetonitrile (Riedel-de Haën, Germany) were also used as received. Deionized water was used throughout the experimental process, prepared using a Milli-Q water system (Milli-Q, resistivity 18.2 MΩ cm). Decamethylferrocene (ABCR, Switzerland) was purified by sublimation producing a highly crystalline solid. High purity CO_2 (>99.998%, CarbaGas, Gümligen) was used in all experiments.

2.2. Equipment

The high-pressure reactor, employed for the electrochemical investigation of DMFc in supercritical CO_2, was built in-house and consisted of a stainless steel cell equipped with a single sapphire window (Rayotek, USA). The reactor was sealed with a stainless steel electrochemical cap consisting of three electrodes. The electrochemical cell consisted of a silver quasi-reference electrode (qRE), a platinum counter electrode and an interchangeable gold disc electrode (geometric area 0.0173 cm^2) set in a PEEK body. The temperature was controlled by a water circulation system surrounding the reactor, thermostated externally to ±0.2 °C. The reactor pressure was monitored using a piezoelectric pressure sensor (Swagelok, UK). CO_2 was introduced and compressed in the reactor using a piston pump (Teledyne Isco, model 100-DX, USA) until the desired pressure was attained.

All electrochemical experiments were performed using a PalmSens portable potentiostat (Ivium Technologies, The Netherlands) with adapted connections. MALDI mass spectrometry was performed on a microflex MALDI-TOF instrument (Bruker Daltonics) and ion chromatography was performed on a Basic IC plus system (Metrohm, Switzerland).

2.3. Synthesis of electrolyte salts

The room temperature ionic liquid (RTIL), used as a lipophilic electrolyte in the subsequent electrochemical experiments, was synthesized by ion exchange of two commercially available precursor salts. The anion was introduced from lithium tetrakis(pentafluorophenyl)borate ($TFPB^-$) and the cation from tetradecyl ammonium bromide (TDA^+). Equimolar solutions of the salts (0.05 mM), each in a 6 : 1 molar ratio of methanol to water, were slowly added together under stirring. The combined solutions were left stirring for 12 hours, at which point a highly viscous gel had formed at the base of the vessel. The methanol–water mixture was discarded and the gel dissolved in 1,2-dichloroethane (DCE). The liquid was then purified by water extraction to remove excess bromide, a process monitored using liquid chromatography. On complete extraction of bromide the DCE and water were vacuum evaporated to leave a viscous, clear liquid. The salt was characterized by MALDI-MS.

2.4. Electrochemical experiments

Prior to the electrochemical investigations the volume of the reactor containing the electrode cap was determined to be 18 ± 0.5 mL. The electrolyte and DMFc concentrations were calculated with respect to the total reactor volume. A pre-determined volume of deoxygenated acetonitrile (0–8 mL) was also added to the reactor along with a magnetic stirrer. The reactor was immediately capped with the three-electrode cap, and a slow flow of CO_2 was passed through the cell whilst the water bath temperature increased to 313 ± 0.2 K (40 °C), taking no more than 5 minutes, and was promptly sealed at the autoclave valve.

On thermal equilibration the CO_2 slowly filled the chamber to a pressure of *ca.* 50 bars (the pressure of the source gas canister). CO_2 was then forced into the reactor using the piston pump until the desired pressure was attained.

Electrochemical experiments were performed at variable scan rates and under quiescent conditions (*i.e.* not stirring). The electrodes were positioned at their closest possible proximity to each other, no more than 5 mm, to decrease uncompensated resistance through the solution.

2.5. Numerical simulations

The voltammetry at a disk-shaped electrode was simulated using finite element method (FEM) computations at the interface of COMSOL Multiphysics 3.5a running on Linux Ubuntu 8.04 platform with a four core Mac Pro (2.66 GHz CPU each) equipped with 9.8 GB RAM. The Fick's diffusion equation in transient form,

$$\frac{\partial c}{\partial t} + \nabla(-D\nabla c) = 0$$

was solved for a two-dimensional computational domain asymmetric with respect to the z axis assuming the diffusion of species with $D = 1.86 \times 10^{-9}$ m^2 s^{-1} (determined from experimental data). The electrode radius was set to 742 μm, corresponding to the Au electrode radius used in the experiments, and the domain width was adapted to have no influence on the results. Assuming reversible kinetics the concentration of oxidized and reduced species at the electrode surface would follow the Nernst relation

$$E = E^{0\prime} + \frac{RT}{F}\ln\left(\frac{c_{DMFc^+}}{c_{DMFc}}\right)$$

where c_{DMFc} and $c_{DMFc}{}^+$ denote the concentration of species at the electrode surface, while F, E, $E^{0\prime}$, R and T specify Faraday's constant, applied potential, standard formal potential (taken as 0 V), gas constant and temperature, respectively. The other

boundary conditions were set to the bulk concentration boundary conditions (c_{bulk} = 0.5 mM), insulation ($-D\nabla c = 0$) and axial symmetry.

The mesh size was refined down to the value of 0.5 μm at the electrode boundary. The transient computations were performed using direct solver UMFPACK with a relative error tolerance of 10^{-5} and an absolute tolerance of 10^{-6} with time stepping taken from the solver. The numerical model was validated using the analytical expression for a Nernstian electrochemical process

$$i = FAc^*\left(\frac{\pi DF}{RT}\nu\right)^{0.5}\chi$$

with i, A and χ, respectively, denoting the measured current, electrode area and the dimensionless function of an applied potential difference. The results for numerical modelling and the analytical solution, for linear diffusion to a planar electrode, were in very good agreement (the relative deviation from analytical result did not exceed 0.5%).

3. Results and discussion

3.1. Conductivity in supercritical CO_2

As discussed in the Introduction, a number of researchers have achieved discernable conductivity in supercritical CO_2 using highly fluorinated and bulky electrolytes. Recent publications by Bartlett *et al.*[14–16] explored a variety of lipophilic electrolytes for use in the supercritical medium, and specifically applied tetrabutylammonium hexafluorophosphate ($TBAPF_6$), tetrabutylammonium tetrafluoroborate ($TBABF_4$) and tetrabutylammonium tetrakis(3,5-trifluoromethyl phenyl)borate (TBATFMPB) as electrolytes for metal electrodeposition in $scCO_2$ fluid, the latter exhibiting the best conductivity. Studies by Abbott *et al.*[5,6,17] during the late 1990's found that increasing the cation size also gave favourable results with respect to the lipophilicity of the salt and solubility in supercritical CO_2 and non-polar solvents. Consequently, the electrolyte used in the present investigation was the large tetra(decyl)ammonium cation (TDA) and tetrakis(pentafluorophenyl)borate anion (TFPB). The synthesis of the salt was reported in a previous publication[20] and is also detailed in the present Experimental section. The bulky electrolyte formed was found to be a room temperature ionic liquid (RTIL), with a melting point of approximately 25 °C, an unusual property given the symmetry of both ions. Nonetheless, similar RTILs have been reported by Samec *et al.*[21] in recent years.

In the presence of no other solvents, the molten electrolyte was found to swell slightly as the CO_2 pressure increased but under supercritical conditions (critical point 73.3 bar, 31.1 °C) a biphasic system was observed. Furthermore, the DMFc also present in the reactor failed to fully mix with either medium, and the solution remained transparent and colourless at the final pressure of 100 bar and a temperature of 40 °C. At pressures below 140 bar, the DMFc was not expected to fully dissolve in the $scCO_2$ however. The TDATFPB–$scCO_2$ fluid did not give a significant current response over a 4 V potential window, and was therefore considered to be non-conducting.

Fig. 1 The mixture of TDATFPB, DMFc and 6 mL of CH_3CN in the supercritical reactor at increasing pressures (*i.e.* concentration of CO_2) and a temperature of 313 K. Two of the electrodes can be seen at the back of the reactor.

Abbott and Harper[5] found that the similar electrolyte salt used in their experimental set-up did dissolve in the $scCO_2$ medium, but at a pressure of 300 bar and a temperature of 70 °C. However, on replicating these conditions, the electrolyte used here did not dissolve, and the discernable current was not observed.

Previous literature regarding electrochemistry in $scCO_2$ and improving solubility in the medium has suggested the use of polar co-solvents such as water,[7] acetonitrile[14–16] and methanol.[14,22] The TDATFPB and DMFc were therefore dissolved in varying amounts of acetonitrile to give a transparent yellow liquid. The liquid readily dissolved in the $scCO_2$, preceded by extensive expansion of the solvent phase during the CO_2 saturation stage, a well-known phenomenon in organic solvents.[18,19] In Fig. 1 these transitions are shown at increasing pressure for 6 mL (*ca.* 30% vol.) CH_3CN. At 10 bar the acetonitrile phase with DMFc and electrolyte is evident in the lower half of the reactor's viewing window. At 47 bar the saturated phase has swollen significantly, though the CO_2 is still gaseous. Finally at 100 bar there appears to be a single phase in the reactor consisting of supercritical CO_2, acetonitrile, DMFc and electrolyte. The transition to the bulk single phase was monitored through the sapphire window and observed from the CO_2 critical point (*ca.* 73 bar), however electrochemical experiments were undertaken at 100 bar and 313 K to ensure supercritical conditions and a reasonably fixed mole ratio of CO_2 to acetonitrile.

In the $scCO_2$–CH_3CN–TDATFPB–DMFc solution a significant current response was observed on the μA scale. The electrolyte concentration was 10 mM and the DMFc concentration 0.5 mM in the final volume of the reactor (18 mL). The volume of acetonitrile added to the reactor was varied between 0.5 and 8 mL corresponding to a mole ratio of CH_3CN–CO_2 of 0.04 to 0.60, respectively, at 100 bar and 313 K. To account for the absorption of the CO_2 by the acetonitrile, and the volume occupied by the co-solvent, exact determination of the CO_2 volume was achieved upon decompression of the reactor. This was found to follow very closely to the initial assumption of a single-phase volume of CO_2 and a mole ratio based on the density of CO_2 at 100 bar and 313 K in the reactor volume. Furthermore, the ionic liquid electrolyte was found not to influence the mole ratio. The CH_3CN–TDATFPB–DMFc mixture did not dissolve in the $scCO_2$ until a ratio of at least 0.07 was achieved, and appreciable solution conductivity was not observed until a mole ratio of 0.13 (2 mL) was used, corresponding well to

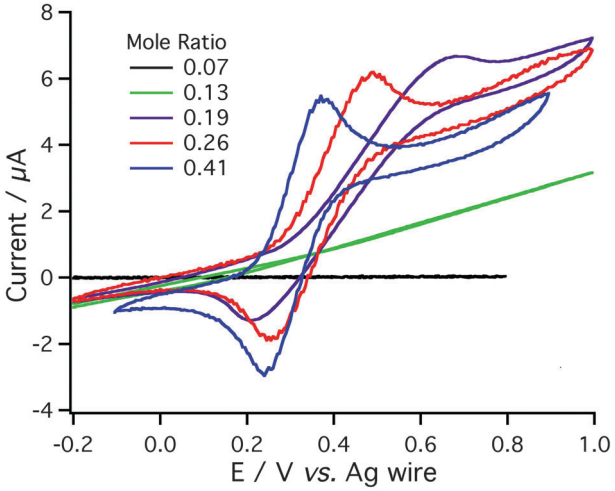

Fig. 2 Overlay of cyclic voltammograms for increasing mole ratios of CH_3CN–CO_2. The solution in each experiment contained 10 mM TDATFPB electrolyte and 0.5 mM DMFc. The scan rate is 200 mV s^{-1}.

literature values.[14,22,23] From a ratio of 0.19 the DMFc redox couple became discernable, however, after a mole ratio of 0.3 any improvement in the DMFc voltammetry was not significant. The variation in voltammetry observed with an increase in mole ratio of CH_3CN–$scCO_2$ is shown in Fig. 2. In the absence of any electrolyte, a redox couple for DMFc was not observed, even at ratios as high as 0.8 (*i.e.* 10 mL).

Despite some degree of uncompensated resistance, the redox couple for DMFc was evident at *ca.* 0.3 V (*vs.* Ag qRE). The voltammetric behaviour shown in Fig. 2 is similar to the response of a rotating disc electrode in a fully supported acetonitrile solution. The measured current is the sum of a steady-state component indicative of a fixed diffusion layer thickness, and of a peak shape response attributed to semi-infinite linear diffusion. As the mole ratio of CH_3CN–CO_2 was increased, the steady state component decreased indicating a thicker diffusion layer. Indeed, extrapolation of the "limiting current" gave a diffusion layer thickness of 39, 54 and 59 μm for 0.19, 0.26 and 0.41 mole ratio, respectively, at 200 mV s^{-1} (estimated using the value of diffusion coefficient established in Section 3.2 *vide infra*, and the calculation $\delta = (FDcA)/i_{lim}$).

Conductivity studies of the TDATFPB electrolyte in acetonitrile at 40 °C show an increase from 100 μS cm^{-1} to 10 mS cm^{-1}. It would appear that this intrinsic conductivity increase sufficiently raises the conductivity of the supercritical CO_2 and acetonitrile mixed fluid, thuseliminating themigrational flux component, and allowing near reversible voltammetry at 0.3 mole ratio and above. As the most peak-shaped voltammetry was achieved after a mole ratio of 0.41, scan rate dependence experiments were performed in this composition.

3.2 The scan rate dependence of DMFc in CH_3CN and $scCO_2$–CH_3CN

The scan rate dependence experiments, shown in Fig. 3a, indicate a semi-infinite linear diffusion process. Using the reversible

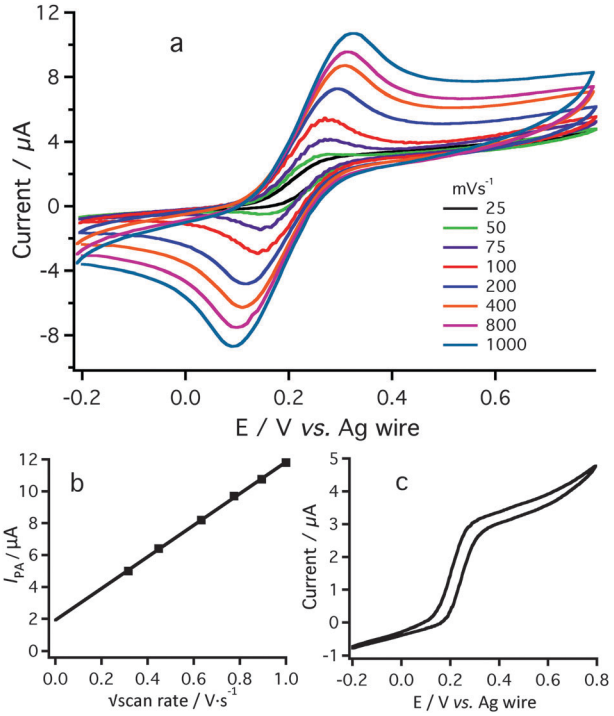

Fig. 3 (a) Overlay of cyclic voltammograms obtained for DMFc at increasing scan rates (25–1000 mV s^{-1}). Medium consists of DMFc (0.5 mM), TDATPFB (10 mM), CH_3CN (mole ratio 0.41) and CO_2 at 100 bar (10 MPa) and 313 K. (b) Plot of anodic peak current *vs.* the square root of the scan rate. (c) The steady-state CV observed at 25 mV s^{-1}.

Randles–Sevcik equation, a linear plot was obtained with R^2 = 0.9995. However, extrapolation to zero scan rate yielded a steady-state component of 2 μA (Fig. 3b). The near steady-state voltammetry observed at 25 mV s^{-1}, illustrated in the inset of Fig. 3a, gave a comparable limiting current of 2.4 μA. A steady-state response was also readily achieved at considerably higher scan rates (1 V s^{-1}), when the system was placed under moderate stirring using a magnetic stirrer.

The electrochemical response of the same three-electrode set-up was also observed in just acetonitrile and electrolyte. In this experiment, the DMFc and electrolyte remained at 0.5 mM and 10 mM, respectively, in the 18 mL of acetonitrile (the total reactor volume) at a temperature of 313 K and a pressure of 1 bar, *i.e.* normal atmospheric pressure. As expected, typical peak-shaped voltammograms attributed to semi-infinite linear diffusion were observed at a macro electrode under quiescent conditions at 25 mV s^{-1} and above. Furthermore, extrapolation of the scan rate dependence plot yielded zero current at zero scan rate, confirming the absence of any steady-state component (Fig. 4). The comparison of CH_3CN and $scCO_2$–CH_3CN voltammetry clearly indicates an intrinsic difference in mass transport regimes, especially as the magnitude of the Faradaic current under both conditions is the same.

Randles–Sevcik analysis of the results shown in Fig. 3 and 4 also allowed for the estimation of the DMFc diffusion coefficient, *D*. The calculated value of 1.86 × 10^{-5} cm^2 s^{-1} under supercritical conditions was almost the same as in just the

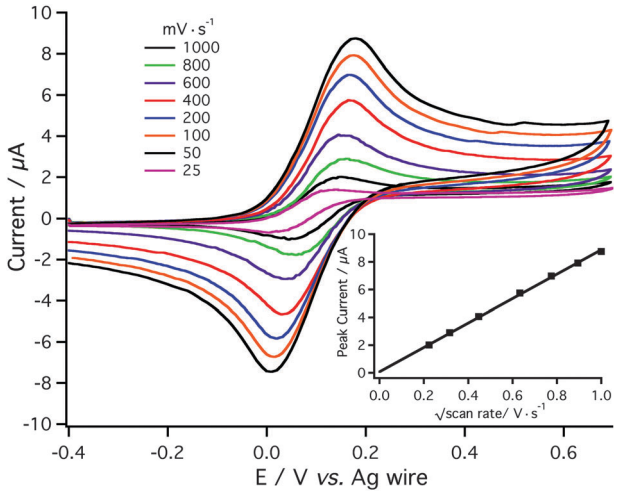

Fig. 4 Overlay of cyclic voltammograms obtained for DMFc (0.5 mM) at increasing scan rates (25–1000 mV s^{-1}) in CH_3CN fully supported by TDATFPB (10 mM), at 313 K. Inset: the plot of anodic peak current *vs.* square root of the scan rate.

acetonitrile (1.85×10^{-5} cm^2 s^{-1}) at the same temperature and concentration of electrolyte. The data are in good agreement with the previously reported constant for DMFc measured in acetonitrile,[24] when the higher temperature of 313 K and different electrolytes used are taken into consideration.

3.3. Diffusion in the $scCO_2$–CH_3CN single-phase

As the diffusion coefficients calculated for DMFc under both conditions are near identical, it would suggest that a liquid-like acetonitrile phase is formed at the electrode surface. The thickness of this layer is restricted under the supercritical conditions, giving rise to a steady-state response at moderate scan rates below 50 mV s^{-1}. From the near steady-state voltammogram observed at 25 mV s^{-1} in the $scCO_2$–CH_3CN solution, a diffusion layer thickness of 60 μm was determined from the limiting current. Given the strict limits of the diffusion layer in the $scCO_2$ fluid, it may be inferred that beyond the liquid-like phase is a more turbulent, supercritical-like phase. This bulk phase exhibits high natural convection, owing to the low viscosity of the supercritical fluid, and inevitable density differences throughout. Compton *et al.*[25,26] observed a comparable steady-state response at macro electrodes in a series of studies exploring sonoelectrochemistry. The exhibited restriction in diffusion layer thickness was much more pronounced in their studies however, ranging between 1 and 6 μm.[26]

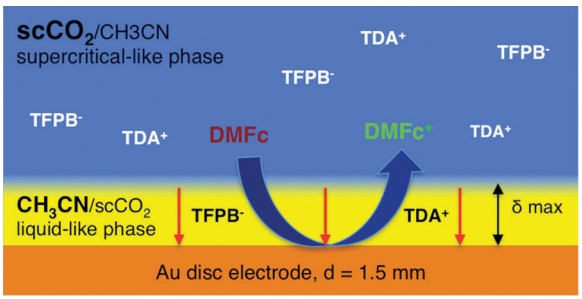

Fig. 5 A schematic representation of the proposed thin-layer of CH_3CN (yellow) compressed and restricted by the more turbulent bulk $scCO_2$–CH_3CN phase (blue). The electrolyte and DMFc concentrations are considered uniform throughout the two liquids, and the diffusion layer thickness is assumed not to propagate beyond the thin layer of CH_3CN.

The electrochemical system may therefore be considered in terms of both thin-layer and convective-diffusion voltammetry. The proposed system is depicted in Fig. 5 with a thin layer of mostly acetonitrile at the electrode surface restricted in thickness by the $scCO_2$–CH_3CN phase in the bulk solution, both of which are fully supported by the electrolyte. The DMFc concentration is uniform throughout the reactor, and supplements the liquid CH_3CN thin layer on depletion of the diffusion layer. Consequently, the diffusion coefficient calculated is that of DMFc in pure acetonitrile and electrolyte, rather than in a more mixed and diffuse solution with $scCO_2$, which would have different viscosity and density.

When electrochemical reactions are performed at a macro interface (*i.e.* at an electrode over a mm in diameter) in a liquid medium the key limitation on the current magnitude is the rate of mass-transport. Typically, when voltammetry is carried out in a large volume of stagnant liquid a depletion of redox species concentration occurs near the electrode surface limiting the measured currents and imposing a concentration gradient towards the electrode. The rate of mass transport is considered entirely dependent on this gradient and the rate at which the redox species can diffuse to the electrode from the bulk concentration. At high scan rates, diffusion limited mass transport effects are particularly pronounced. In contrast, in well-stirred or convective media the rate of redox species consumption at the electrode is comparable to the fast mass transfer rate to the electrode, thus providing a constant, steady flux of material for oxidation or reduction (*i.e.* steady-state). The intermediate case with a thin layer of stagnant liquid phase, between an electrode and highly convective solution, should exhibit transitional behavior.

3.4. Computational studies of the proposed system

To confirm this hypothesis finite element simulations were used to compute currents at a disk electrode as a function of applied potential difference at a given scan rate (ν). The voltammetry at a disk-shaped electrode was simulated using finite element method (FEM) computations of a two-dimensional domain. The model assumed that mass-transport of the redox species followed the transient form of Fick's diffusion equation

$$\frac{\partial c}{\partial t} + \nabla(-D\nabla c) = 0$$

with Nernstian kinetic behavior at the electrode (see Experimental section). The outer boundary of the axisymmetric computational domain was assumed to be a highly convective medium where the concentration of redox species remained constant at the bulk value throughout the supercritical reactor. Two specific conditions were explored. The first simulated the

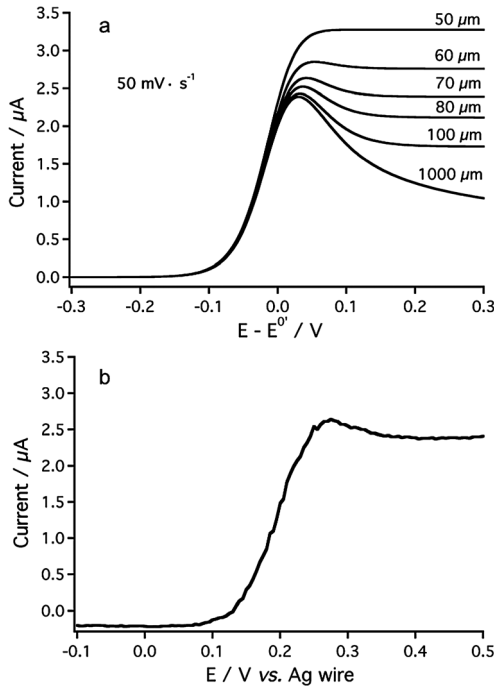

Fig. 6 (a) Overlay of simulated linear sweep voltammograms in which the scan rate is fixed at 50 mV s^{-1} but the thin layer thickness is varied. (b) The baseline corrected forward scan of the experimental data was obtained at 50 mV s^{-1}.

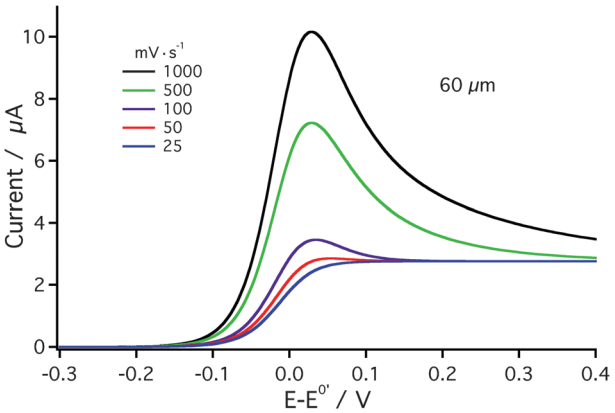

Fig. 7 An overlay of simulated linear sweep voltammograms in which the thin layer thickness is fixed at 60 μm and the scan rate is varied.

response at a fixed scan rate but varying thin layer thickness, whereas the second simulation varied the scan rate against a fixed thin layer depth.

Fig. 6a depicts the effect of the thickness, l, of a liquid-like domain formed at the electrode, *i.e.* the transition between mass-transport regimes due to a decrease in l value. As can be seen, the plateau of "limiting current" appears when this liquid-like layer is in the order of a few hundred microns and the steady-state sigmoidal-like voltammogram is observed when the thin layer thickness decreases down to 50 μm. Most likely, the mass-transport governing factor is the ratio between the diffusion layer thickness δ, which is always established near the electrode during voltammetric experiments, and the size of the quiescent liquid-like phase. Evidently, when l is thin enough to be comparable with the diffusion domain size δ, mass-transport to the electrode is maintained by redox species arriving from the bulk phase. In other words, the diffusion layer is not able to propagate over this liquid boundary, which supplies molecules to the depleted region at the electrode.

The experimental evidence suggests a thin-layer thickness of 60 μm. The simulated voltammogram at 50 mV s^{-1} in Fig. 6a does indeed reflect the transitional voltammetry observed in Fig. 3 at the same scan rate (*i.e.* the onset of diffusion limited voltammetry on a sigmoidal steady-state current) at a thickness between 60 and 70 μm. The baseline corrected experimental data at 50 mV s^{-1} are shown in Fig. 6b to aid comparison of the simulated and real data. Simulations were also conducted with a liquid-like layer of fixed thickness, equal to 60 μm, at different scan rates as shown in Fig. 7. At low and moderate potential scan rates up to 500 mV s^{-1} the plateau of limiting current could be observed, while at higher scan rates the diffusion of redox species becomes relatively sluggish in comparison with the rapidly changing voltage perturbation. Under such conditions, the diffusion field δ is unable to expand enough to be comparable with l, and the typical peak-shaped voltammogram is observed. Again, these computational results are evidently in very good agreement with the experimental data, corroborating the existence of an approximately 60 μm thick acetonitrile film at the electrode surface.

4. Conclusions

These experiments have shown that electrochemistry can be performed in supercritical CO_2, without the aid of enhanced convection, microelectrode dimensions or a modified electrode surface. The use of a lipophilic ionic liquid electrolyte and polar co-solvent has overcome the conductivity problems associated with the non-polar supercritical fluid, providing a fully supported single-phase for electrochemical investigation.

The low viscosity supercritical carbon dioxide fluid evidently enhances diffusion into the electrode, as steady-state voltammetry is observed at high scan rates of up to 50 mV s^{-1}. Moderate stirring of the solution also gave near steady-state voltammetry at scan rates as high as 1000 mV s^{-1}. Experimental and simulation results suggest that a quiescent liquid-like film of mostly CH_3CN and electrolyte is formed at the electrode surface, which is limited in thickness but supplemented by a more convective, supercritical-like phase in the bulk solution. The presence of this film enables electrochemical studies of species dissolved in the supercritical phase. This opens new avenues to study the reactivity of CO_2 by electrochemical methods, and provides invaluable information for electrodeposition processes and electrosynthetic methods in the supercritical CO_2 medium.

Acknowledgements

The authors would like to thank the NCCR MUST program and Swiss National Science Foundation (SNSF) for financial support.

We would also like to thank Liang Qiao for his help with mass spectrometry, and Valerie Devaud for ever-present laboratory support.

Notes and references

1 M. Gattrell, N. Gupta and A. Co, *J. Electroanal. Chem.*, 2006, **594**, 1–19.
2 M. E. Philips, M. R. Deakin, M. V. Novotny and R. M. Wightman, *J. Phys. Chem.*, 1987, **91**, 3934–3936.
3 E. F. Sullenberger and A. C. Michael, *Anal. Chem.*, 1993, **65**, 2304–2310.
4 H. Ohde, F. Hunt, S. Kihara and C. M. Wai, *Anal. Chem.*, 2000, **72**, 4738–4741.
5 A. P. Abbott and J. C. Harper, *J. Chem. Soc., Faraday Trans.*, 1996, **92**, 3895–3898.
6 A. P. Abbott and J. C. Harper, *Phys. Chem. Chem. Phys.*, 1999, **1**, 839–841.
7 D. Niehaus, M. Philips, A. Michael and R. M. Wightman, *J. Phys. Chem.*, 1989, **93**, 6232–6236.
8 A. C. Michael and R. M. Wightman, *Anal. Chem.*, 1989, **61**, 270–272.
9 A. C. Michael and R. M. Wightman, *Anal. Chem.*, 1989, **61**, 2193–2200.
10 S. Chanfreau, P. Cognet, S. Camy and J. S. Condoret, *J. Electroanal. Chem.*, 2007, **604**, 33–40.
11 J. Jun and P. S. Fedkiw, *J. Electroanal. Chem.*, 2001, **515**, 113–122.
12 P. Vanysek and V. Novak, *ECS Trans.*, 2009, **19**, 55–63.
13 M. A. Mendez, R. Partovi-Nia, I. Hatay, B. Su, P. Ge, A. Olaya, N. Younan, M. Hojeij and H. H. Girault, *Phys. Chem. Chem. Phys.*, 2010, 12.
14 P. N. Bartlett, D. C. Cook, M. W. George, J. Ke, W. Levason, G. Reid, W. Su and W. Zhang, *Phys. Chem. Chem. Phys.*, 2010, **12**, 492–501.
15 D. Cook, P. N. Bartlett, W. Zhang, W. Levason, G. Reid, J. Ke, W. Su, M. W. George, J. Wilson, D. Smith, K. Mallik, E. Barrett and P. Sazio, *Phys. Chem. Chem. Phys.*, 2010, **12**, 11744–11752.
16 J. Ke, W. Su, S. M. Howdle, M. W. George, D. Cook, M. Perdjon-Abel, P. N. Bartlett, W. Zhang, F. Cheng, W. Levason, G. Reid, J. Hyde, J. Wilson, D. C. Smith, K. Mallik and P. Sazio, *Proc. Natl. Acad. Sci. U. S. A.*, 2009, **106**(14768–14772), S14768.
17 A. P. Abbott, T. A. Claxton, J. Fawcett and J. C. Harper, *J. Chem. Soc., Faraday Trans.*, 1996, **92**, 1747–1749.
18 S. Chanfreau, P. Cognet, S. Camy and J. S. Condoret, *J. Supercrit. Fluids*, 2008, **46**, 156–162.
19 Y. Houndonougbo, B. B. Laird and K. Kuczera, *J. Chem. Phys.*, 2007, **126**, 074507–074508.
20 A. J. Olaya, M. A. Méndez, F. Cortes-Salazar and H. H. Girault, *J. Electroanal. Chem.*, 2010, **644**, 60–66.
21 Z. Samec, J. Langmaier and T. Kakiuchi, *Pure Appl. Chem.*, 2009, **81**, 1473–1488.
22 W. Wu, W. Li, B. Han, T. Jiang, D. Shen, Z. Zhang, D. Sun and B. Wang, *J. Chem. Eng. Data*, 2004, **49**, 1597–1601.
23 W. Wu, J. Zhang, B. Han, J. Chen, Z. Liu, T. Jiang, J. He and W. Li, *Chem. Commun.*, 2003, 1412–1413.
24 M. Matsumoto and T. W. Swaddle, *Inorg. Chem.*, 2004, **43**, 2724–2735.
25 K. B. Holt, J. Del Campo, J. S. Foord, R. G. Compton and F. Marken, *J. Electroanal. Chem.*, 2001, **513**, 94–99.
26 R. G. Compton, F. Marken and T. O. Rebbitt, *Chem. Commun.*, 1996, 1017–1018.

